



**HAL**  
open science

## Melarsoprol-cyclodextrins inclusion complexes.

Stéphane Gibaud, Siham Ben Zirar, Pierre Mutzenhardt, Isabelle Fries, Alain Astier

► **To cite this version:**

Stéphane Gibaud, Siham Ben Zirar, Pierre Mutzenhardt, Isabelle Fries, Alain Astier. Melarsoprol-cyclodextrins inclusion complexes.. International Journal of Pharmaceutics, 2005, 306 (1-2), pp.107-21. 10.1016/j.ijpharm.2005.09.003 . hal-00399630

**HAL Id: hal-00399630**

**<https://hal.science/hal-00399630>**

Submitted on 6 Oct 2016

**HAL** is a multi-disciplinary open access archive for the deposit and dissemination of scientific research documents, whether they are published or not. The documents may come from teaching and research institutions in France or abroad, or from public or private research centers.

L'archive ouverte pluridisciplinaire **HAL**, est destinée au dépôt et à la diffusion de documents scientifiques de niveau recherche, publiés ou non, émanant des établissements d'enseignement et de recherche français ou étrangers, des laboratoires publics ou privés.

## MELARSOPROL-CYCLODEXTRINS INCLUSION COMPLEXES

Stéphane Gibaud\* , Siham Ben Zirar, Pierre Mutzenhardt, Isabelle Fries, Alain Astier

*Laboratoire de Pharmacie Clinique, EA 3452, Faculté de Pharmacie. 5, rue Albert Lebrun,  
54000 Nancy, FRANCE.*

\*Corresponding author: S. GIBAUD

Laboratoire de Pharmacie Clinique – EA 3452

5, rue Albert Lebrun –BP 403

54001 Nancy Cedex

France

Tel: + (33) 3 83 68 23 10

Fax: + (33) 3 83 68 23 07

e-mail: [stephane.gibaud@pharma.uhp-nancy.fr](mailto:stephane.gibaud@pharma.uhp-nancy.fr)

**ABSTRACT**

Melarsoprol, a water-insoluble drug, is mainly used in the treatment of trypanosomiasis and has demonstrated an *in vitro* activity on myeloid and lymphoid leukemia derived cell lines. It is marketed as a very poorly tolerated non-aqueous solution (Arsobal®). The aim of our work was to develop melarsoprol/cyclodextrin complexes in order to improve the tolerability and the bioavailability of Melarsoprol. Phase-solubility analysis showed A<sub>L</sub>-type diagrams with β-cyclodextrin (βCD), randomly methylated β-cyclodextrin (RAMEβCD) and hydroxypropyl-β-cyclodextrin (HPβCD), which suggested the formation of 1:1 inclusion complexes. The solubility enhancement factor of melarsoprol (solubility in 250 mM of cyclodextrin / solubility in water) was about  $7.2 \times 10^3$  with both β-cyclodextrin derivatives. The 1:1 stoichiometry was confirmed in the aqueous solutions by the UV spectrophotometer using Job's plot method. The apparent stability constants  $K_{1:1}$ , calculated from mole-ratio titration plots, were  $57\,143 \pm 4\,425 \text{ M}^{-1}$  for RAMEβCD and  $50\,761 \pm 5\,070 \text{ M}^{-1}$  for HPβCD. Data from <sup>1</sup>H NMR and ROESY experiments provided a clear evidence of inclusion complexation of melarsoprol with its dithiaarsane extremity inserted into the wide rim of the cyclodextrin torus. Moreover, RAMEβCD had a pronounced effect on the drug hydrolysis and the dissolution rate of melarsoprol. However, the cytotoxic properties of melarsoprol on K562 and U937 human leukemia cell lines was not modified by complexation.

**Keywords:** melarsoprol; methylated-β-cyclodextrin; hydroxypropyl-β-cyclodextrin; complexation; nuclear magnetic resonance; cytotoxicity

## 1. INTRODUCTION

The human African trypanosomiasis (sleeping sickness), transmitted by the tsetse flies, is a daily threat to more than 60 million people in 36 countries of sub-Saharan Africa. The estimated number of persons thought to be affected by the disease is between 300,000 and 500,000, which creates a major health problem. The trypanosomiasis is considered as one of the most neglected diseases by the World Health Organization, which urges to increase the research efforts and considers that optimizing the efficacy, the safety, and the simplicity of drug regimens administration should be favored, including the reformulation of old, but effective, drugs (WHO, 2002).

Until now, the only effective drug available for the late-stage treatment of trypanosomiasis is the trypanocidal melarsoprol (Mel). An As<sup>III</sup> organoarsenic drug, which was introduced in the 50's by Freidhem ([Friedheim, 1949](#)). Moreover, recent studies showed that Mel is also very effective in the treatment of several refractory leukaemia (Rivi et al., 1996; Konig et al., 1997; [Soignet et al., 1999](#)) and could be an attractive alternative to the arsenious oxide which has recently been approved for the treatment of these severe blood disorders.

Mel, a very poorly water soluble drug, was dissolved in propylene glycol at 3.6% to develop the only commercially available solution (Arsobal<sup>®</sup>, Aventis Pharma). In addition to the severe systemic toxicities caused by the drug substance, this non-aqueous solution exhibits a local intolerability (severe pains, burns, and necrosis) and must always be administered by slow intravenous injection thus, requiring a professional hospital care. Therefore, this treatment remains very difficult to use in emerging countries, particularly in the field, which restricts its availability. Furthermore, no oral forms of this drug were ever developed.

For several years, the modified CDs have been used as solubilizing agents. Among the industrially produced  $\beta$ -cyclodextrin derivatives, the most important ones are the highly water-soluble methylated  $\beta$ -cyclodextrin and hydroxypropylated- $\beta$ -cyclodextrin. Randomly

methylated- $\beta$ -cyclodextrin (RAME $\beta$ CD) is marketed in non-parenteral formulations (e.g. Aerodio<sup>®</sup>, 17 $\beta$ -estradiol, Servier, France and Clorocil<sup>®</sup>, chloramphenicol, Oftalder, Portugal). Nevertheless, RAME $\beta$ CD cannot be used in parenteral formulations; because of its affinity to cholesterol is so strong that it extracts cholesterol from the blood cell membranes, resulting in hemolysis in around 1 mg/mL. On the contrary, hydroxypropyl  $\beta$ -cyclodextrin (HP $\beta$ CD) was marketed in oral (e.g. Sporanox<sup>®</sup>, Itraconazole, Janssen, USA) and i.v. formulations (MitoExtra<sup>®</sup>, mitomycin, Novartis, Switzerland).

Recently, one modified CD (sulfobutylether- $\beta$ -cyclodextrin, Captisol<sup>®</sup>) was used as a solubilizing agent to obtain parenteral formulations of two newly approved drugs; the antifungal voriconazole ([Donnelly and De Pauw, 2004](#)) and the anti-schizophrenia agent, ziprasidone (Kim et al, 1998).

The most interesting property of cyclodextrins (CDs) is their ability to form inclusion complexes with a large variety of apolar and hydrophobic molecules. Their use was extensively exploited to improve the pharmaceutical properties of numerous drugs such as water solubility, stability, physicochemical incompatibilities, oral absorption or to modulate biological activity ([Frömming and Szejtli, 1994](#); [Al-Omar et al., 1999](#); [Garcia-Rodriguez et al., 2001](#)). Thus, we have studied the advantages of employing the CDs to develop an oral form and a parenteral aqueous solution of MeI, which could improve the tolerability and the safety of the drug.

## 2. MATERIALS AND METHODS

### 2.1. Materials:

Melarsoprol ( $\{2-[4-(4,6\text{-Diamino-[1,3,5]triazin-2-ylamino})\text{-phenyl}]-[1,3,2]\text{dithiarsolan-4-yl}\}$ -methanol; Mel) was synthesized according to the method described by Friedheim (Friedheim, 1942; 1947a; 1947b; 1985). Its chemical structure is presented in Fig.1. The organoarsenic purity was greater than 99% confirmed by the HPLC analysis and its structure was ascertained by  $^1\text{H}$ - and  $^{13}\text{C}$ -NMR. The arsenic percentage, determined by titration with bromate after mineralization, was 18.77% (theoretically: 18.81%). The cyclodextrins [ $\alpha$ -cyclodextrin ( $\alpha$ -CD),  $\beta$ -cyclodextrin ( $\beta$ CD), hydroxypropyl- $\beta$ -cyclodextrin (substitution degree = 4.4; HP $\beta$ CD), randomly methylated- $\beta$ -cyclodextrin (1.6-2.0 methyl unit per anhydroglucose unit; RAME $\beta$ CD) and dimethyl- $\beta$ -cyclodextrin (DM $\beta$ CD)] were purchased from Sigma-Aldrich (Saint-Quentin, France). In all experiments, the water content of the CDs was determined by coulometric Karl-Fisher method, and then the weighed mass of the CDs was adjusted accordingly. All other reagents were of analytical grade from either Merck Eurolab (Fontenay-sous-Bois, France) or Acros organics (Noisy-le-Grand, France) and were used as received.

### 2.2. Melarsoprol assays:

Determinations of the included Mel were carried out by the high performance liquid chromatography (HPLC) or the ultra-violet spectrophotometer (UV) after dissociation by an initial dilution with pure dimethylsulfoxide (DMSO); the appropriate final adjustments were performed with distilled water.

For HPLC determinations, 50  $\mu\text{l}$  sample was injected onto a  $\text{C}_{18}$  column (5  $\mu\text{m}$ , 4.6 x 25 cm, Macherey-Nagel, Eckbolsheim, France) using an autosampler (WISP 712, Waters). The mobile phase was a mixture of acetonitrile and 6% acetic acid in water (23/77; v/v) at a flow rate of 1.5 ml/min (SP8800 pump, Spectra Physics, TSP, CA). Detection was

performed by UV spectrophotometer at 286 nm (Waters 490E detector) using a SP-800 integrator (Spectra Physics). The method was linear up to 500  $\mu\text{g/ml}$  with a detection limit  $< 0.1 \mu\text{g/ml}$ . As previously described, chromatograms and  $^1\text{H}$  NMR spectra showed that Mel contains two isomers (ratio 3:1) as a result of the slow inversion of the trivalent arsenic pyramidal configuration ([Ericsson et al., 1997](#)).

For UV determinations, after suitable dilutions, the samples were measured in a 1-cm cell using a Carry 50 spectrophotometer (Varian, les Ulis, France). Standard curves were constructed under identical conditions.

### **2.3. Phase solubility studies of melarsoprol complexation with $\alpha\text{CD}$ , $\beta\text{CD}$ , RAME $\beta\text{CD}$ and HP $\beta\text{CD}$ :**

Mel complexation with various cyclodextrins was evaluated using the phase-solubility method ([Higuchi and Connors, 1965](#)). A suspension of a large excess of Mel (30 mg) in 2 ml of aqueous solutions of the appropriate CD (concentrations ranging from 10 to 250 mM, pH adjusted to 7) was stirred in screw-capped amber vials during 24 hours on a rock-and-roller agitator at 25°C. Under these conditions, the solution mostly contained the non-ionized Mel [ $\text{pK}_a = 4.8$ , ([Keiser and Burri, 2000](#))] and no significant degradation of the drug was observed. Preliminary “time-dependence” experiments showed that the equilibrium was reached after this stirring period. Each suspension was then centrifuged at 9000  $\times g$  for 5 min, diluted from 1/200 to 1/500 with DMSO and water (final DMSO concentration:  $10^{-2}$  to  $10^{-3}$ ; v/v) and the amount of dissolved Mel was assessed by HPLC or UV at 280 nm.

The apparent solubility of the substrate ( $[\text{Mel}]_{\text{tot}}$ ) was determined as a function of the added ligand concentration ( $[\text{CD}]_{\text{tot}}$ ) ([Frömming and Szejtli, 1994](#)). Since the phase solubility diagrams were of  $A_L$ -type and assuming a 1:1 complex, the apparent stability (or

formation) constant  $K_a$  was calculated for each CD using the slope from the linear regression analysis of the phase-solubility isotherm using the following equation:

$$K_a = \frac{\text{slope}}{S_0 \cdot (1 - \text{slope})} \quad (\text{Eq.1})$$

The inherent solubility of Mel ( $S_0$ ) was determined in pure water under identical conditions. The determinations were performed in triplicate and the constants were expressed as the mean  $\pm$  SD.

## 2.4. Characterization of Mel complexes:

The phase solubility studies allowed us to select two  $\beta$ CD derivatives (RAME $\beta$ CD and HP $\beta$ CD) for further experiments.

### 2.4.1. Liquid phase analysis of RAME $\beta$ CD/Mel and HP $\beta$ CD/Mel

#### 2.4.1.1. Continuous variation (Job's plot) method

Stock solutions of Mel were prepared at  $2.5 \times 10^{-5}$  M in 0.1% (v/v) and 1% (v/v) DMSO/water mixtures and at  $1.25 \times 10^{-5}$  M in water. The complex Mel/CD was formed at a constant volume by adding various concentrations of either CD dissolved in the respective solvent at several molar ratios  $r = [\text{Mel}] / ([\text{Mel}] + [\text{CD}])$ , varying from 0.1 to 0.9 to reach a final total molarity of  $2.5 \times 10^{-5}$  M or  $1.25 \times 10^{-5}$  M. The absorbance of the solution was monitored at 280 and 286.6 nm. The absorbance difference  $\Delta A = A_0 - A$  was determined by measuring the absorbance of Mel with (A) and without ( $A_0$ ) cyclodextrin at each wavelength in a 1-cm path length cell thermostated at  $25 \pm 1^\circ\text{C}$ . The product  $\Delta A \times [\text{Mel}]$  versus  $r$  was then plotted to determine the stoichiometry of the complex which was 1:1 when  $\Delta A \times [\text{Mel}]$  reached its maximum for  $r=0.5$ .

As melarsoprol is insoluble in pure water, this experiment was previously performed with 0.1% (v/v) and 1% (v/v) DMSO/water mixtures to ascertain the negligible influence of DMSO at low concentrations.



### 2.4.1.2. Spectroscopic determination of binding constants

The mole-ratio titration method was used to confirm the values of  $K_a$  estimated by the phase-solubility isotherms ([Yoe and Jones, 1944](#); [Benesi and Hildebrand, 1949](#); [Dotsikas et al., 2000](#)). Various amounts of RAME $\beta$ CD or HP $\beta$ CD solutions were added in fixed aliquots to a Mel solution ( $2.5 \cdot 10^{-5}$  M in 1% (v/v) DMSO/water mixture), leading to Mel/CD ratio varying from 1/5 to 1/100. In preliminary experiments, the absorbance of each vial was measured, time-dependently, up to 10 min to assess the kinetics of the complex.

At each time, the total absorbance  $A_t$  in a 1-cm cell was given by:

$$A_t = \epsilon_{\text{Mel}} \times [\text{Mel}]_t + \epsilon_{\text{CD}} \times [\text{CD}]_t + \epsilon_{\text{Mel:CD}} \times [\text{Mel/CD}]_t \quad (\text{Eq. 2})$$

where  $[\text{Mel}]_t$ ,  $[\text{CD}]_t$  and  $[\text{Mel/CD}]_t$  are the respective concentrations of the species at time  $t$ ,  $\epsilon_{\text{Mel}}$ ,  $\epsilon_{\text{CD}}$  and  $\epsilon_{\text{Mel:CD}}$  are the molar absorptivities with units of  $\text{mol}^{-1}\text{cm}^{-1}$  and  $\Delta\epsilon_{1:1} = \epsilon_{\text{Mel:CD}} - \epsilon_{\text{Mel}} - \epsilon_{\text{CD}}$ .

Since  $[\text{Mel}]_{\text{tot}} = [\text{Mel}]_t + [\text{Mel/CD}]_t$ , a combination of Eq.2 with the definition of the binding constant of the 1:1 inclusion complex ( $K_{1:1} = [\text{Mel/CD}]_t / [\text{Mel}]_t [\text{CD}]_t$ ) results in Eq.3:

$$\Delta A = \frac{[\text{Mel}]_{\text{tot}} \cdot K_{1:1} \cdot \Delta\epsilon_{1:1} \cdot [\text{CD}]_t}{1 + K_{1:1} [\text{CD}]_t} \quad (\text{Eq.3})$$

where  $\Delta A = A_t - A_0$ .

The binding constants were obtained from the titration curve data ( $\Delta A$  as a function of  $[\text{CD}]_t$ ) fitted by non-linear regression (Eq.3, Graph Pad Software, Synergy Inc, Pasadena).

### 2.4.2. Solid phase analysis of Mel/RAME $\beta$ CD and Mel/HP $\beta$ CD

The solid phase analysis of the complexes was performed on lyophilized samples. Mel (30 mg;  $7.5 \times 10^{-5}$  mol) was stirred (25°C; 24 h) in 10 ml of distilled water containing RAME $\beta$ CD or HP $\beta$ CD and filtered through a 0.22  $\mu\text{m}$  membrane filter (Millipore HA, 0.22  $\mu\text{m}$ ). The filtrate was freeze dried and stored at + 4°C until use.

#### 2.4.2.1. X-ray diffraction (XRD)

Powder X-ray diffraction patterns were obtained with D500 Siemens diffractometer system with Co  $K\alpha$  radiation ( $\lambda=1.78897 \text{ \AA}$ ) over the interval  $10-45^\circ/2\theta$ . The measurement conditions were as follows: target, Co; filter, Fe; voltage 35 kV; current 20 mA.

#### 2.4.2.2. Differential Scanning Calorimeter (DSC)

The DSC thermograms were obtained on a scanning calorimeter (Pyris, Perkin Elmer Instruments, St Quentin, France). The instrument was calibrated using indium as a standard. Samples (5 mg) were heated in sealed aluminium pans under nitrogen using the following program: hold for 10 min at  $40.0^\circ\text{C}$ ; heat from  $40.0^\circ\text{C}$  to  $250.0^\circ\text{C}$  at a scanning rate of  $10^\circ\text{C}/\text{min}$ .

#### 2.4.3. Determination of the complex structure by $^1\text{H}$ NMR measurements

All experiments were performed on a Bruker Avance DRX NMR spectrometer operating at 9.4 Tesla (proton frequency: 400.133 MHz) and at a sample temperature of 300 K. The 2D-ROESY experiments were recorded with the following parameters: mixing times 300 ms with a radiofrequency field of 8 kHz, acquisition map 2K x 256, number of scans 16. Final 2D-map after FT: 1K x 1K.

The lyophilized MeI/RAME $\beta$ CD and MeI/HP $\beta$ CD complexes, obtained as previously described, were dissolved in  $\text{D}_2\text{O}$ . For solubility reasons, the spectrum of free MeI was obtained in  $\text{d}_6$ -DMSO. Chemical shifts were given in part per million (ppm) relative to the solvent signal (HOD at 4.84 ppm). Since the commercial RAME $\beta$ CD used in all experiments contained 1.6 – 2.0 methyl unit per anhydroglucose and does not have a defined composition,  $^1\text{H}$ -NMR spectra were carried out using a complex obtained with pure heptakis (2,6-di-O-methyl)-  $\beta$ -cyclodextrin (DM $\beta$ CD) substituted at the primary (O-6) and at the secondary (O-2) hydroxyl groups.

#### 2.4.4. Pharmaceutical properties of Mel/ RAME $\beta$ CD complex

##### 2.4.4.1. Dissolution kinetics

In order to investigate the relative dissolution kinetics, the dispersed amount method was used. One mg of free melarsoprol or an equivalent amount of the lyophilized Mel/RAME $\beta$ CD complex powder was suspended in a mixture of 70 ml of phosphate buffer (0.1 M, pH 7.40) and 30 ml of propylene glycol preheated to 37°C. The suspensions were incubated, at 37°C, in a shaking-bath, 200 strokes/min (Heito, France). One ml aliquots were taken at various intervals up to 24 h and centrifuged (7200 x g, 5 min, Denver Instruments, MA). The supernatants were then analyzed by HPLC in order to assess their drug contents. The results are presented as mean  $\pm$  SD of triplicate experiments. The resulting dissolution curves were analyzed in terms of the dissolved drug percentage (DP<sub>t</sub>) and the dissolution efficiency (DE<sub>t</sub>) according to the equation:

$$DE = \frac{\int_0^t D dt}{D_{100t}} \times 100 \quad (\text{Eq.4})$$

where D is the percentage of the dissolved drug at time t and D<sub>100t</sub> is the area of the rectangle corresponding to a total dissolution (100%) at the same time (Khan, 1975; Naidu et al, 2004).

##### 2.4.4.2. Stability studies

Pure Mel or Mel/RAME $\beta$ CD complex were suspended in 0.1 M phosphate buffer at pH 7.0 to obtain 4  $\mu$ g/ml solutions (expressed in Mel), poured into screw-capped vials and incubated at 25, 37 or 60°C ( $\pm$  1°C) in a shaking-bath, 200 strokes/min (Heito, France). At various intervals ranging from 1 to 72 hours, 50  $\mu$ l of the solution were set apart and analyzed by HPLC. The first-order rate constant for the degradation of the drug is the weight average of 2 rate constants, where (K<sub>f</sub>) and (K<sub>c</sub>) are the pseudo-first order rate degradation constants for the hydrolysis of free or totally included melarsoprol

respectively,  $F_f$  is the fraction of free drug in solution and  $[\text{Mel}]_t$  is the free drug concentration at time  $t$  (Loftsson, 1996, Dotsikas 2002).

$$\frac{d[\text{Mel}]_t}{dt} = -K_{obs}[\text{Mel}]_t \quad (\text{Eq.5}) \quad \text{and} \quad K_{obs} = K_f F_f + K_c [1 - F_f] \quad (\text{Eq.6})$$

The constants were determined kinetically by non-linear regression from the plots of the percentage of the remaining drug ( $\%_{\text{mel}}$ ) as a function of time ( $t$ ), according to  $\%_{\text{mel}} = 100.e^{-Kt}$ . The respective activation energies for the degradation were obtained from the Arrhenius plots [ $\ln K_f = f(1/T)$  or  $\ln K_c = f(1/T)$ ].

#### 2.4.4.3. *In vitro* cytotoxicity on K 562 and U937 cell lines

The cytotoxic activity of Mel and Mel/RAME $\beta$ CD complex was performed on K562 and U937 human leukemia cell lines. Briefly, exponential growing cells were seeded into a 12-well plate at a density of  $0.2 \times 10^6$ /well. Triplicate wells contained Mel or Mel/RAME $\beta$ CD at concentrations ranging from 1.25 to 50  $\mu\text{M}$ . The cells were incubated for 2 or 3 days at 37°C in a humidified 5% CO<sub>2</sub> atmosphere. Cell densities were determined by a duplicate cell count using a haemocytometer. Cells that excluded trypan blue dye (L; living cells) were counted and compared to those of the control culture (C) in order to assess the growth inhibition percentage using  $(L/C) \times 100$ . Cells that did not exclude the dye (D; dead cells) were also counted and compared to the total number of cells in the well (T) to assess the mortality percentage calculated by  $(D/T) \times 100$ . Cellular viability was also estimated by the lysosomal coloration method using neutral red dye (Borenfreund et Puerner, 1984). For each concentration tested, 4 wells were used, then the mean value was calculated. For each parameter (growth inhibition and mortality percentage), the corresponding EC<sub>50</sub> (effective concentration for 50 % of the maximum response  $A_{\text{max}}$ ) was calculated by non-linear fitting of the experimental data using a sigmoidal dose response model according to the equation:

$$A_C = \frac{A_{\max}}{1 + 10^{(\log EC_{50} - \log C)}} \quad (\text{Eq. 7})$$

where  $A_C$  is the response for the concentration  $C$  (GraphPad, Prism Software).

### 3. RESULTS AND DISCUSSION

Since the complexes obtained with RAME $\beta$ CD (Mel/RAME $\beta$ CD) and HP $\beta$ CD (Mel/HP $\beta$ CD) gathered the best solubility enhancement factor, their physicochemical properties were investigated in details. The hypothesis of 1:1 stoichiometry of the inclusion complexes was confirmed by the continuous variation method (Job's plot) and their respective apparent stability constants in solution were studied by the mole-ratio titration method using the UV spectrophotometer. The formation of a true inclusion complex between Mel and RAME $\beta$ CD was also demonstrated by the differential scanning calorimeter (DSC) and the X-ray diffractometer (XRD) in the solid state after freeze-drying. Furthermore,  $^1\text{H}$  NMR spectra, two-dimensional rotating frame nuclear Overhauser effect spectroscopy (2D-ROESY) experiments were carried out to confirm the hypothesized inclusion mode of Mel/RAME $\beta$ CD.

Finally, additional properties of Mel/RAME $\beta$ CD complex such as drug stability, dissolution profiles and efficacy were studied to demonstrate the suitability of the complexation to develop acceptable pharmaceutical forms.

#### 3.1. Phase solubility of melarsoprol with $\alpha$ CD, $\beta$ CD, RAME $\beta$ CD and HP $\beta$ CD

Mel is a lipophilic compound ( $\log P = 2.53$ ), which is very poorly soluble in water:  $S_0 = 6 \text{ mg.l}^{-1}$  at  $25^\circ\text{C}$  ( $1.25 \times 10^{-5} \text{ M}$ ).  $\alpha$ CD did not significantly improve the solubility of Mel; this is probably due to the lack of incorporation of the Mel in the small cavity of  $\alpha$ CD (internal diameter: 0.57 nm). On the opposite,  $\beta$ CD and its modified derivatives, which have an internal diameter of 0.68 nm, showed a better solubilization of Mel. The parent molecule  $\beta$ CD exhibited a steeply linear phase-solubility diagram (Fig. 2, inset) but the amounts of dissolved Mel were rapidly limited by the poor solubility of the complex, which

precipitated after about 2 mM of added CD. Thus, a B-type phase-solubility diagram, according to Higuchi and Connors classification, was obtained.

The Mel/RAME $\beta$ CD and Mel/HP $\beta$ CD isotherms (Fig. 2) were linear within the CD concentration range studied, corresponding to an A<sub>L</sub>-type profile with a slope less than 1 and indicating that the inclusion complexes could be of the first order with respect to the CDs (1:1 stoichiometry). The apparent stability constants  $K_a$  were  $56\,077 \pm 4\,205\text{ M}^{-1}$  for Mel/RAME $\beta$ CD and  $54\,168 \pm 5\,350\text{ M}^{-1}$  for Mel/ HP $\beta$ CD.

These close values of binding constants suggest that the solubilization process is identical between these  $\beta$ CD derivatives, regardless of the substitution of the external hydroxyl groups of the toroidal shape. However, it was demonstrated that the slope of the phase-solubility diagram in a drug/cyclodextrin system could be linear in spite of the enhanced solubility occurring through both inclusion and non-inclusion processes such as complex aggregates or micellar formation ([Loftsson et al., 2002](#)). Thus, an A<sub>L</sub>-type isotherm does not necessarily demonstrate the formation of an inclusion complex and other experiments are required to ascertain the process. Nevertheless, the complexation efficiency of these CDs, as defined by the product  $S_0 \cdot K_{1:1}$  ([Loftsson et al., 1999](#); [Loftsson et al., 2002](#)), was about 0.67. The solubility enhancement factor, as defined by the ratio of the solubility of Mel in 250 mM solution of CD to its inherent solubility  $S_0$ , was about  $7.2 \times 10^3$  for both CDs. This interesting finding is coherent with the well-admitted principle claiming that the less the aqueous solubility of the pure drug, the greater the relative solubility enhancement by the CD complexation ([Loftsson and Brewster, 1996](#)). [Sharma et al. \(1995\)](#) showed that the enhancement factor for the highly lipophilic anticancer drug paclitaxel varied from  $2.3 \times 10^3$  for HP $\beta$ CD to  $9.9 \times 10^4$  for DM $\beta$ CD. Interestingly, despite the fact that the HP $\beta$ CDs are generally considered as less effective solubilizers than the randomly methylated derivatives, the enhancement factor is similar for both CDs in our case.

Considering the excellent solubilizing properties of RAME $\beta$ CD and HP $\beta$ CD for Mel, which led to the formation of complexes with apparent stability constants in the range considered as optimal for pharmaceutical uses ([Loftsson and Brewster, 1996](#)), we decided to profoundly investigate the physicochemical and pharmaceutical properties of these complexes.

### 3.2. Stoichiometry and binding constant of Mel/RAME $\beta$ CD and Mel/HP $\beta$ CD

In aqueous or 1% (v/v) aqueous DMSO solution, Mel exhibited a maximum absorbance at 280 nm mainly due to the conjugation of the 3,5-diamino triazine ring with the benzene nucleus (molar absorption coefficient  $\epsilon_{\text{mel}} = 10\,916 \pm 105 \text{ M}^{-1}\cdot\text{cm}^{-1}$ ;  $n=5$ ). The titration of Mel with increasing concentrations of RAME $\beta$ CD and HP $\beta$ CD (up to a *ratio* CD/Mel=100) showed a concentration-dependant bathochromic effect leading to a maximum shift to 286.6 nm, a CD-dependent increase of absorbance at this wavelength (hyperchromic shift) and an isosbestic point at 277 nm are in good accordance with the supposed complexation, by inclusion, process (Fig.3). However, when the chromophore part of a guest molecule is inserted into a CD cavity, an opposite behavior is more frequently observed (hypsochromic and hypochromic shifts). Thus, the bathochromic and hyperchromic shifts could suggest that the 4,6-diamino triazine ring is not inserted into the cavity. Furthermore, these shifts could be linked to an extended conjugation of the respective  $\pi$  electrons of both aromatic rings due to a stabilizing interaction between the triazine ring and the outside part of the CD core.

Time-dependent experiments showed a rapid stabilization of absorbance (< 2 min) after the addition of CDs indicating a rapid in solution complexation (data not shown). Moreover, the absorbance remained stable for several hours.

The continuous variation method (Job's plot) was used to confirm the inclusion process and the 1:1 stoichiometry as suggested from solubility experiments. The difference  $\Delta A$  was



measured at 280 and 286.6 nm for mixtures of Mel and both CDs in water and 0.1% (v/v) DMSO/water mixture with the total molarity remaining constant. Fig. 4 represents the 2<sup>nd</sup> order-polynomial fitted curves of  $\Delta A \times [\text{Mel}]$  as a function of  $r = [\text{Mel}] / ([\text{Mel}] + [\text{CD}])$  ( $r > 0.999$ ;  $n=3$ ). Thus, these Job's plots demonstrate that, since  $\Delta A \times [\text{Mel}]$  is maximum at  $r$  value of 0.5, both complexes have a 1:1 stoichiometry. Identical results were obtained for both wavelengths and regardless of the solvent. However, a better correlation coefficient and reproducibility were noticed when we used 0.1% (v/v) DMSO in water.

The stability constants  $K_{1:1}$ , were also calculated from the molar-ratio titration plots by non-linear regression (Fig. 5) and were  $57\,143 \pm 4\,425 \text{ M}^{-1}$  for RAME $\beta$ CD and  $50\,761 \pm 5\,070 \text{ M}^{-1}$  for HP $\beta$ CD ( $n=3$ ). These values were very close to those obtained from phase-solubility experiments. Thus, these results suggest the formation of a soluble 1:1 inclusion complex, though the presence of adsorbed molecules, which kept their spectral characteristics, could not be excluded.

It was demonstrated that the relative error of the Benesi-Hildebrand method (*i.e.* double reciprocal treatment of titration data) in measuring the association constants of CD complexations is often poorly reliable except for the  $K$  values  $\leq 1\,000 \text{ M}^{-1}$  (Salvatierra et al., 1997; [Yang et al., 2000](#)). Since the complexation of Mel was strong, a non-linear regression estimation of the binding constants was chosen. For all experiments, the estimation error of binding constants, determined as the midpoint of the hyperbolic fitting of an individual set of experimental data, was less than 10 %.

### 3.3. Characterization of solid Mel/RAME $\beta$ CD and HP $\beta$ CD complexes

The DSC and the XRD are widely used to study the complexation by CDs in the solid state. Therefore, these analytical methods were used to ascertain the inclusion process in solid complexes obtained by freeze-drying.

The DSC profile of RAME $\beta$ CD exhibited a large endothermic event from 90 to 140°C, attributed to the evaporation of the absorbed water, followed by an endothermic peak at 181°C corresponding to its melting point whereas the melting point of Mel occurred at 221°C. The DSC profile of the two raw materials, compared to the thermogram of the Mel/RAME $\beta$ CD, confirms that there was a real inclusion of the Mel into the RAME $\beta$ CD. In fact, the formation of an inclusion complex is suggested by the absence of both melting endotherms in the DSC thermogram of the complex, as previously described for other drugs such as  $\beta$ -blockers ([Ficarra et al., 2000](#)) or zolpidem ([Trapani et al., 2000](#)). The DSC profile of Mel/HP $\beta$ CD was very similar to this of Mel/RAME $\beta$ CD.

The XRD also demonstrated the formation of an amorphous inclusion complex between RAME $\beta$ CD and Mel. The diffractogram of pure Mel exhibited numerous peak characteristics of its crystalline form, while RAME $\beta$ CD showed only a broad amorphous band. The diffraction pattern of the freeze-dried complex showed that the drug had lost its crystalline state, and the small residual peaks were attributed to minute amounts of non-included Mel.

### 3.4. Determination of complexes geometry by NMR determinations

NMR spectroscopy is known to be one of the most useful methods to obtain information about the geometry of inclusion complexes ([Djedaini et al., 1990](#); [Ganza-Gonzalez et al., 1994](#); [Kim et al., 2004](#)). The  $^1\text{H}$  NMR peak assignments for free and complex Mel are reported in Table 1, where the corresponding shifts are  $\Delta\delta = \delta(\text{complex}) - \delta(\text{free})$ . According to the previously published study by [Ericsson et al \(1997\)](#), the two

diastereoisomeric forms of Mel, due to the slow inversion of the pyramidal structure of the trivalent arsenic, were observed at the expected 3:1 ratio. These isomers can be clearly identified by the different chemical shifts of the respective aromatic AA'BB' coupling system (Figs. 6 and 7). It has been suggested that the orientation of the CH<sub>2</sub>OH group of the dithiaarsane ring is pseudoaxial, the major isomer A has R in pseudoequatorial (*trans*) position and the minor B isomer has R in pseudoaxial (*cis*) position (Fig. 7).

In the presence of CDs, most of the Mel protons were strongly upfield shifted (Table 1). No new peaks were observed in the spectrum, indicating a dynamic exchange process between the free and the included state during the NMR time scale ([Loukas et al., 1997](#)). Both conformational isomers were similarly shifted; however, the isomeric *ratio* was strongly modified by the complexation since the minor isomer, which represented 25 % in free Mel, was decreased to about 5%, as estimated by integration (Fig.6). This fact could suggest a preferential inclusion of the major *trans* isomer and thus, a shift of the inversion equilibrium toward the *trans* isomer. The largest upfield shifts were observed for H-d and H-b protons indicating that the dithiaarsane ring undergo a significant perturbation upon complexation. Moreover, the H-e benzene protons, located near the Ar-As bond, were also strongly shifted whereas the H-f protons were only slightly perturbed. These facts strongly suggest that the complexation process involves the dithiaarsane extremity of the molecule. As Ganza-Gonzalez et al (1994) previously described, these upfield shifts of the Mel protons could be due to an interaction with the  $\pi$  electrons of the oxygen atoms of the CD. The <sup>1</sup>H chemical shifts of DM $\beta$ CD in the absence and the presence of Mel are shown in Table 2. The peak assignments obtained with the DM $\beta$ CD used throughout the experiments were in good agreement with those previously reported. As expected, the H-3 and H-5 protons located inside the cavity and the protons from the external H-6 group at the narrower extremity were significantly shifted. These findings proved the existence of an interaction between the guest molecule and the interior of the CD cavity, confirming our

hypothesis of the inclusion mode. The H-1 protons located at the exterior of the torus were also affected suggesting a possible adsorption of melarsoprol on the outside surface of the cyclodextrin.

Mel/RAME $\beta$ CD and Mel/DM $\beta$ CD ROESY experiments (Fig. 8) showed an intense correlation between the internal H-3 and H-5 protons of the CD, which could suggest that the aromatic ring is deeply inserted into the CD (Fig. 9). However, the H-2 and H-4 of these CDs were also correlated with the aromatic ring of the Mel and it was assumed that some Mel molecules were adsorbed, contributing to the solubility increase. These CDs contain substituted methyl groups, thus became more hydrophobic and therefore adsorb, more effectively, the melarsoprol.

### **3.5. Melarsoprol stability in Mel/RAME $\beta$ CD**

The formation of an inclusion complex between Mel and RAME $\beta$ CD has a pronounced stabilizing effect on the drug decomposition. Actually, It has been previously shown that Mel is not a stable compound and samples stored for long periods of time should be kept at -70°C and protected from humidity ([Ericsson et al., 1997](#)). The main degradation process is a general acid-base catalyzed hydrolysis leading to an opening of the dithiaarsane ring with the formation of melarsenoxide. ([Berger and Fairlamb, 1994](#); [Loiseau et al., 2000](#)). Thus, the influence of the complexation by cyclodextrins on the stability of Mel was studied using the Mel/RAME $\beta$ CD complex. The degradation kinetics of Mel and the complex were performed at 25°C, 37°C and 60°C and the quantification of Mel degradation was carried out from the data obtained by HPLC. This degradation follows a temperature-dependant first order process and was significantly lower for the included Mel than for the free drug since the stability's half-life was doubled as showed by the respective pseudo-first-order constants  $K_f$  and  $K_c$  (Table 3).

The Arrhenius plot in the presence of RAME $\beta$ CD was parallel to that in its absence, indicating that the degradation mechanism remained essentially the same (data not shown). The mean activation energy  $E_a$  for Mel degradation was 77.87 kJ.M<sup>-1</sup> and, after complexation, it increased to 80.80 kJ.M<sup>-1</sup> leading to a difference of + 3.07 kJ.M<sup>-1</sup> ( $P < 0.01$ ). A similar increase of  $E_a$  was previously described in the protection of insulin hydrolytic deamidation by complexation with RAME $\beta$ CD ([Dotsikas and Loukas, 2002](#)).

Our results demonstrate a protecting effect of CD on the Mel degradation. Sure enough, it is well known that the complexation of hydrolysis-sensitive drugs by the CDs might affect their stability by retardation or acceleration of the degradation process, depending on the inclusion mode. ([Loftsson and Brewster, 1996](#)). Our results were also coherent with the geometry of the complex postulated from the NMR experiments. Indeed, the insertion of the dithiaarsane ring into the hydrophobic cavity of the CD limits the access of water molecules and, thus, decreases the hydrolysis rate.

### **3.6. Dissolution study of Mel/RAME $\beta$ CD complex**

One of the aims of this work was to develop an oral form of Mel using the formation of an inclusion complex with RAME $\beta$ CD. Therefore, the dissolution profile was a key pharmaceutical parameter to investigate. Figure 10 illustrates the dissolution profile obtained with pure Mel and Mel/RAME $\beta$ CD. Since the inherent solubility of melarsoprol was too low to respect sink conditions in an aqueous solution, the dissolution study was performed in a mixture of phosphate buffer 0.1 M, pH 7.4 (70 ml) and propylene glycol (30 ml). Even in these conditions, which strongly favor the dissolution of the drug alone, the dissolution rate of the complex was significantly higher than this of the free Mel. The respective dissolution parameters are presented in table 4. As compared to free Mel, a very rapid and total dissolution of the complex was observed. The dissolution efficiency after 10 min  $DE_{10}$  was  $24.6 \pm 2.0$  for the free drug and  $96.7 \pm 2.5$  for the included drug ( $P <$

0.0001). The dissolution was total for the complex after 60 min whereas only  $60.3 \pm 6.1\%$  of the free Mel was dissolved. These results demonstrate that the solubility properties of Mel are dramatically improved by its complexation with RAME $\beta$ CD.

### 3.7. *In vitro* cytotoxicity of Mel/RAME $\beta$ CD on K562 and U937 cell lines

The growth inhibition of cells exposed to Mel/RAME $\beta$ CD was similar to that of free Mel as estimated by the trypan blue dye exclusion method (Table 5). However, the mortality rates after 2 days exposure to Mel/RAME $\beta$ CD were less than those obtained with free Mel ( $TM_{50} = 20.87 \mu\text{M}$  vs  $5.25 \pm 0.38 \mu\text{M}$ ;  $P < 0.01$ ), but became equivalent in the third day of incubation. In U937 cell line, the growth inhibition was slightly reduced at T+72h ( $3.16 \pm 0.07 \mu\text{M}$  vs  $2.40 \pm 0.02 \mu\text{M}$ ;  $p < 0.01$ ), but was not different for K562 cells. Similar values were obtained using the neutral red dye test to assess the viability (data not shown).

These results could be explained by the protection of Mel from hydrolysis by its complexation and the consequent slower transformation to melarsenoxide, formed by simple hydrolysis, which represents the active metabolite of melarsoprol (Cristau and Placidi, 1972; Cristau et al., 1972). Melarsenoxide was synthesized by Friedheim in 1939, used for several years (Friedheim, 1948) and then abandoned because of its toxicity. Recently, Keiser et al (2000) showed that melarsenoxide undergoes further transformation into one or more active compounds that still contain the arsenic moiety. However, the toxicity of melarsoprol has not been differentiated from the toxicity of melarsenoxide and is probably considerably less active. Indeed, the mechanism of the covalent binding and the reactive groups of the proteins are unknown but the formation of a Schiff base with the parasitic trypanothione (Fairlamb, 1990) was proposed as well as the formation of covalent links with cysteinyl residues of proteins (Van Schaftingen et al., 1987). However, after 3 days of incubation, most of Mel was totally hydrolyzed to melarsenoxide, which explains why the cytotoxicity difference became insignificant. Nevertheless, our results suggest that the complexation of Mel by RAME $\beta$ CD or HP $\beta$ CD do not impair its pharmacological activity.

## 4. Conclusion

Our results demonstrate that the very poorly soluble drug melarsoprol forms 1:1 inclusion complexes with  $\beta$ CD and its derivatives, especially RAME $\beta$ CD and HP $\beta$ CD. The solubilization enhancement factor by  $\beta$ CD is limited but could be multiplied by a factor of about  $7.2 \times 10^3$  using RAME $\beta$ CD and HP $\beta$ CD. The stability constants determined by the solubility method and the UV spectrophotometer are high and in good agreement for both methods, suggesting that inclusion was the essential mode of complexation. Their values are also closely related for both CDs suggesting a similar inclusion process. This solubility enhancement is interesting especially with the low-toxic derivative HP $\beta$ CD and could be considered in a possible development of a suitable aqueous-based i.v. formulation.

When compared to the pure drug, the dissolution profile of the Mel/RAME $\beta$ CD complex is dramatically improved, which proved its suitability to develop an oral form.  $^1\text{H}$  NMR experiments in solution also confirmed the formation of the complexes and demonstrated an insertion of the *trans* isomer of Mel with its dithiaarsane extremity into the wide rim of the CD cavity. This geometry might explain the increased resistance of Mel to hydrolysis in its complexed form. However, as demonstrated by *in-vitro* experiments on a model of human cancer cell lines, the cytotoxic efficacy of the drug is not modified by the complexation. Further works are in progress to study the oral bioavailability of Mel/RAME $\beta$ CD on animal models and to assess the expected improvement of local tolerability of a potential newly HP $\beta$ CD-based i.v. form of this drug.



**Acknowledgments**

This work was supported by a generous grant from the French National Institute for Medical Research (INSERM, CreS n° 4CR04F) and by the University Henri Poincaré, Nancy, under grant BQR 2003.

We thank Pr. P. Mutzenhardt and Pr. D. Canet “Service Commun de RMN, Université Henri Poincaré Nancy 1, Faculté des Sciences, BP 239, 54506 Vandœuvre-lès-Nancy, France” for their assistance in the NMR measurements and their fruitful discussions.

## References

Al-Omar, A., Abdou, S., De Robertis, L., Marsura, A., Finance, C., 1999. Complexation study and anticellular activity enhancement by doxorubicin-cyclodextrin complexes on a multidrug-resistant adenocarcinoma cell line. Bioorg Med Chem Lett. 9, 1115-1120.

Benesi, H.A., Hildebrand, J.H., 1949. A spectrophotometric investigation of the interaction of iodine with aromatic hydrocarbons. J Am Chem Soc. 71, 2703-2707.

Berger, B.J., Fairlamb, A.H., 1994. Properties of melarsamine hydrochloride (cymelarsan) in aqueous solution. Antimicrob Agents Chemother. 38, 1298-1302.

Cristau, B., Placidi, M., 1972. Routes and kinetics of arsenic elimination in rats after administration of organoarsenic drugs. IV. Biliary excretion of melarsoprol, melarsonyl and related compounds. Med Trop (Mars). 32, 477-482.

Cristau, B., Placidi, M., Audibert, P., 1972. Routes and kinetics of arsenic elimination in rats after administration of organoarsenic drugs. 3. Study of amino-4-benzene arsenic acid and melarsen. Med Trop (Mars). 32, 467-476.

Djedaini, F., Lin, S.Z., Perly, B., Wouessidjewe, D., 1990. High-field nuclear magnetic resonance techniques for the investigation of a beta-cyclodextrin: Indomethacin inclusion complex. J Pharm Sci. 79, 643-646.

Donnelly, J.P., De Pauw, B.E., 2004. Voriconazole a new therapeutic agent with an extended spectrum of antifungal activity. Clin Microbiol Infect. 10, 107-117.

Dotsikas, Y., Kontopanou, E., Allagiannis, C., Loukas, Y.L., 2000. Interaction of 6-p-toluidinylnaphthalene-2-sulphonate with beta-cyclodextrin. J Pharm Biomed Anal. 23, 997-1003.

Dotsikas, Y., Loukas, Y.L., 2002. Kinetic degradation study of insulin complexed with methyl-beta cyclodextrin. Confirmation of complexation with electrospray mass spectrometry and (1)H NMR. J Pharm Biomed Anal. 29, 487-494.

Ericsson, O., Schweda, E.K., Bronner, U., Rombo, L., Friden, M., Gustafsson, L.L., 1997. Determination of melarsoprol in biological fluids by high-performance liquid chromatography and characterisation of two stereoisomers by nuclear magnetic resonance spectroscopy. J Chromatogr B. 690, 243-251.

Fairlamb, A.H., 1990. Future prospects for the chemotherapy of human trypanosomiasis. 1. Novel approaches to the chemotherapy of trypanosomiasis. Trans R Soc Trop Med Hyg. 84, 613-617.

Ficarra, R., Ficarra, P., Di Bella, M.R., Raneri, D., Tommasini, S., Calabro, M.L., Gamberini, M.C., Rustichelli, C., 2000. Study of beta-blockers/beta-cyclodextrins inclusion complex by NMR, DSC, X-ray and SEM investigation. J Pharm Biomed Anal. 23, 33-40.

Friedheim, E.A.H., 1942. Substituted [1,3,5,-triazinyl-(6)]-aminophenyl-arsonic acids and process for manufacture of same, US patent 2 295 574, 15 Sept.

Friedheim, E.A.H., 1947a. Organometallic compounds containing 1,3,5-triazine ring, UK patent GB 585 678, 19 Feb.

Friedheim, E.A.H., 1947b. Substituted 1,3,5-triazyl-(6)-amino-phenyl-arsenic compounds, US patent 2 422 724, 24 June.

Friedheim, E.A.H., 1948. Melarsen oxide in the treatment of human african trypanosomiasis. Ann Trop Med. 42, 357-363.

Friedheim, E.A.H., 1949. Mel B in the treatment of human trypanosomiasis. Am J Trop Med. 29, 173-180.

Friedheim, E.A.H., 1985. Melaminylthioarsenites, US patent 4 514 390, 30 Apr.

Frömming, K.H., Szejtli, J., 1994. Cyclodextrin in pharmacy, Kluwer Academic Publisher, Dordrecht.

Ganza-Gonzalez, A., Vila-Jato, J.L., Anguiano-Igea, S., Otero-Espinar, F.J., Blanco-Mendez, J., 1994. A proton nuclear magnetic resonance study of the inclusion complex of naproxen with [beta]-cyclodextrin. Int J Pharm. 106, 179-185.

Garcia-Rodriguez, J.J., Torrado, J., Bolas, F., 2001. Improving bioavailability and anthelmintic activity of albendazole by preparing albendazole-cyclodextrin complexes. Parasite. 8, S188-190.

Higuchi, T., Connors, K.A., 1965. Phase-solubility techniques. In: C.N. Reilley (Ed.), Advances in Analytical Chemistry and Instrumentation, Vol. 4, Wiley-Interscience, New York, pp 117-212.

Keiser, J., Burri, C., 2000. Physico-chemical properties of the trypanocidal drug melarsoprol. Acta Trop. 74, 101-104.

Keiser, J., Ericsson, O., Burri, C., 2000. Investigations of the metabolites of the trypanocidal drug melarsoprol. Clin Pharmacol Ther. 67, 478-488.

Kim, J.H., Lee, S.K., Ki, M.H., Choi, W.K., Ahn, S.K., Shin, H.J., Hong, C.I., 2004. Development of parenteral formulation for a novel angiogenesis inhibitor, CKD-732 through complexation with hydroxypropyl-[beta]-cyclodextrin. Int J Pharm. 272, 79-89.

Kim, Y., Oksanen, D.A., Masefski, W., Jr., Blake, J.F., Duffy, E.M., Chrnyk, B., 1998. Inclusion complexation of ziprasidone mesylate with beta-cyclodextrin sulfobutyl ether. J Pharm Sci. 87, 1560-1567.

Konig, A., Wrazel, L., Warrell, R.P., Jr., Rivi, R., Pandolfi, P.P., Jakubowski, A., Gabrilove, J.L., 1997. Comparative activity of melarsoprol and arsenic trioxide in chronic B-cell leukemia lines. Blood. 90, 562-570.

Loftsson, T., Brewster, M.E., 1996. Pharmaceutical applications of cyclodextrins. 1. Drug solubilization and stabilization. J Pharm Sci. 85, 1017-1025.

Loftsson, T., Magnusdottir, A., Masson, M., Sigurjonsdottir, J.F., 2002. Self-association and cyclodextrin solubilization of drugs. J Pharm Sci. 91, 2307-2316.

Loftsson, T., Masson, M., Sigurjonsdottir, J.F., 1999. Methods to enhance the complexation efficiency of cyclodextrins. S.T.P. Pharma Sciences. 9, 237-242.

Loiseau, P.M., Lubert, P., Wolf, J.G., 2000. Contribution of dithiol ligands to in vitro and in vivo trypanocidal activities of dithiaarsanes and investigation of ligand exchange in an aqueous solution. Antimicrob Agents Chemother. 44, 2954-2961.

Loukas, Y.L., Vraka, V., Gregoriadis, G., 1997. Novel non-acidic formulations of haloperidol complexed with beta-cyclodextrin derivatives. J Pharm Biomed Anal. 16, 263-268.

Rivi, R., Calleja, E., Konig, A., Lai, L., Gambacorti-Passerini, C., Scheinberg, D., Gabilove, J.L., Warrell, R.P., Pandolfi, P.P., 1996. Organic arsenical melarsoprol shows growth suppressive activity via programmed cell death on apl and other myeloid and lymphoid leukemia derived cell lines. Blood. 88, 68a.

Salvatierra, D., Diez, C., Jaime, C., 1997. Host/guest interactions and NMR spectroscopy. A computer program for association constant determination. J Incl Phenom. 27, 215-231.

Sharma, U.S., Balasubramanian, S.V., Straubinger, R.M., 1995. Pharmaceutical and physical properties of paclitaxel (Taxol) complexes with cyclodextrins. J Pharm Sci. 84, 1223-1230.

Soignet, S.L., Tong, W.P., Hirschfeld, S., Warrell, R.P., Jr., 1999. Clinical study of an organic arsenical, melarsoprol, in patients with advanced leukemia. Cancer Chemother. Pharmacol. 44, 417-421.

Trapani, G., Latrofa, A., Franco, M., Pantaleo, M.R., Sanna, E., Massa, F., Tuveri, F., Liso, G., 2000. Complexation of zolpidem with 2-hydroxypropyl-beta-, methyl-beta-, and 2-hydroxypropyl-gamma-cyclodextrin: Effect on aqueous solubility, dissolution rate, and ataxic activity in rat. J Pharm Sci. 89, 1443-1451.

Van Schaftingen, E., Opperdoes, F.R., Hers, H.G., 1987. Effects of various metabolic conditions and of the trivalent arsenical melarsen oxide on the intracellular levels of fructose 2,6-bisphosphate and of glycolytic intermediates in trypanosoma brucei. Eur J Biochem. 166, 653-661.

WHO, 2002, Human african trypanosomiasis: Treatment and drug resistance network for sleeping sickness., Report of the sixth steering committee meeting.

Yang, C., Liu, L., Mu, T.W., Guo, Q.X., 2000. The performance of the Benesi-Hildebrand method in measuring the binding constants of the cyclodextrin complexation. Anal Sci. 16, 537-539.

Yoe, J.H., Jones, A.L., 1944. Colorimetric determination of Fe with disodium 1,2-dihydroxybenzene-3,5-disulfonate. Ind Eng Chem, Anal Ed. 16, 111-115.

## Figure Legends

Fig. 1: The chemical structure of melarsoprol.

Fig. 2: Phase solubility diagrams of melarsoprol in the presence of RAME $\beta$ CD (-●-), HP $\beta$ CD (-□-),  $\beta$ CD (-■-) and  $\alpha$ CD (-△-) in distilled water at 25°C. Inset: expansion of the initial part of the curves.

Fig. 3. Effect of RAME $\beta$ CD addition on the UV spectra of melarsoprol ( $2.5 \times 10^{-5}$  M in 0.1% (v/v) DMSO/water). The figure shows a concentration-dependent bathochromic shift (280 to 286.6 nm) and a corresponding hyperchromic effect. The solid line arrow indicates the displacement of the curves corresponding to the increasing amounts of CD.

Fig. 4: Continuous variation plot (Job's plot) for the complexation of melarsoprol (Mel;  $2.5 \times 10^{-5}$  M in 0.1% (v/v) DMSO/water) by RAME $\beta$ CD (-●-) and HP $\beta$ CD (-□-).  $\Delta A$ = difference of absorbance at 286.6 nm with (A) and without ( $A_0$ ) cyclodextrin;  $r = [\text{Mel}] / ([\text{Mel}] + [\text{CD}])$ .

Fig. 5: Mole-ratio titration plots of melarsoprol ( $2.5 \times 10^{-5}$  M in 1% (v/v) DMSO/water) by RAME $\beta$ CD (-●-) and HP $\beta$ CD (-□-). The formation of the complex was monitored at 286.6 nm.

Fig. 6: Partial plot of the  $^1\text{H-NMR}$  spectra of free and complexed melarsoprol (Mel) with methyl  $\beta$ -cyclodextrin at 1:5 molar ratio (Mel/RAME $\beta$ CD), corresponding to the benzene ring area. AA' and BB' denote the aromatic coupling system corresponding to the H-e and H-f protons. Mel was dissolved in  $d_6$ -DMSO and Mel/RAME $\beta$ CD in  $\text{D}_2\text{O}$ .

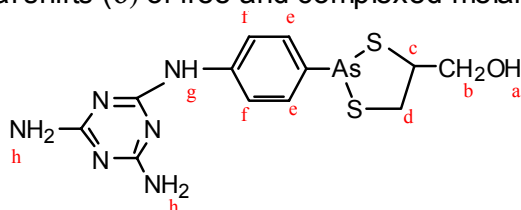


Fig. 7. Conformation of the melarsoprol isomers at the dithiaarsane ring. Major isomer:  $\text{CH}_2\text{OH}_{\text{axial}}$  and  $\text{R}_{\text{axial}}$  (*trans*); Minor isomer:  $\text{CH}_2\text{OH}_{\text{axial}}$  and  $\text{R}_{\text{equatorial}}$  (*cis*)

Fig. 8. Partial contour plot of the two-dimensional ROESY spectrum of melarsoprol (Mel) in the presence of (2,6-di-O-methyl)- $\beta$ -cyclodextrin (DM $\beta$ CD) in  $\text{D}_2\text{O}$ .

Fig. 9. Molecular models of Mel/DM $\beta$ CD derived from 2D ROESY experiments.

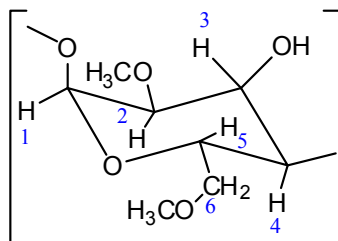
Fig. 10. Dissolution profile of free melarsoprol (-X-) and complexed with methyl  $\beta$ -cyclodextrin (-●-) in a 7:3 mixture of 0.1 M phosphate buffer (pH 7.4) and propylene glycol at 37°C (mean  $\pm$  S.D.; n=3).

Table 1:  $^1\text{H}$  NMR chemical shifts ( $\delta$ ) of free and complexed melarsoprol (Mel);

Proton Type	Melarsoprol		Mel/DM $\beta$ CD			
	Major	Minor	Major		Minor	
	$\delta$ (ppm)		$\delta$ (ppm)	$\Delta\delta$	$\delta$ (ppm)	$\Delta\delta$
a *	5.158	5.158	*	-	*	-
b	2.840	2.791	2.602	-0.238	N.r.	-
c	3.788	3.672	N.r.	-	N.r.	-
d	2.506	2.506	2.153	-0.353	2.153	-0.353
e	7.821	7.838	7.676	-0.145	7.631	-0.207
f	7.490	7.538	7.472	-0.018	7.529	-0.009
g *	8.991	8.991	*	-	*	-
h *	6.320	6.320	*	-	*	-

$\Delta\delta = \delta(\text{complex}) - \delta(\text{free})$ ; Major and minor denotes isomers of melarsoprol (Mel); \* signal disappearing with trace of  $\text{H}_2\text{O}$ ; N.r. = peak non resolved. DM $\beta$ CD = (2,6-di-O-methyl)- $\beta$ -cyclodextrin.

Table 2.  $^1\text{H}$  NMR chemical shifts ( $\delta$ ) of Me $\beta$ CD and MeI/DM $\beta$ CD complex in  $\text{D}_2\text{O}$ . In the formula of glucopyranose unit, R represents H or  $\text{OCH}_3$ .



Proton type	Chemical shift (ppm)		$\Delta\delta$
	DM $\beta$ CD	MeI/DM $\beta$ CD	
H-1	5.172	5.128	-0.044
H-2	N.r.	N.r.	N.d.
H-3	3.944	3.874	-0.070
H-4	3.531	3.508	-0.023
H-5	3.845	3.851	+0.006
H-6	3.721	3.658	-0.063
6-OCH <sub>3</sub>	3.344	3.326	-0.018
2-OCH <sub>3</sub>	3.548	3.522	-0.026

Solutions were made in  $\text{D}_2\text{O}$ . Chemical shifts are given in ppm relative to HOD signal at 4.840 ppm.

$\Delta\delta = \delta(\text{complex}) - \delta(\text{free})$ ; N.r. = not resolved; N.d. = not determined; MeI = melarsoprol; DM $\beta$ CD = (2,6-di-O-methyl)- $\beta$ -cyclodextrin

Table 3: Pseudo-order degradation rate constants and corresponding half-life values for free melarsoprol (Mel) and complexed with methyl  $\beta$ -cyclodextrin (Mel/RAME $\beta$ CD) at 3 different temperatures (mean  $\pm$  S.E.; n=3)

T (°C)	Mel		Mel/RAME $\beta$ CD	
	$K_f$ (h $^{-1}$ )	$T_{1/2}$ (h)	$K_c$ (h $^{-1}$ )	$T_{1/2}$ (h)
25	0.017 $\pm$ 0.009	65.1 $\pm$ 20.8	0.007 $\pm$ 0.001	111.5 $\pm$ 20.2*
37	0.023 $\pm$ 0.006	33.5 $\pm$ 7.5	0.012 $\pm$ 0.005	87.5 $\pm$ 40.5
60	0.378 $\pm$ 0.080	2.0 $\pm$ 0.3	0.133 $\pm$ 0.044	5.6 $\pm$ 0.9*

\*  $P < 0.05$  ( $t$  test)

Table 4: Dissolution parameters of free melarsoprol (Mel) and complexed with methyl  $\beta$ -cyclodextrin (Mel/RAME $\beta$ CD) at 37°C (mean  $\pm$  S.D., n=3). The solubility parameters DE and DP are defined in the experimental section.

Solubility Parameter	Mel	Mel/RAME $\beta$ CD
Dissolution efficiency (%)		
DE <sub>10</sub>	24.6 $\pm$ 2.0	96.7 $\pm$ 2.5*
DE <sub>30</sub>	42.3 $\pm$ 4.0	98.7 $\pm$ 1.5*
Dissolution percent (%)		
DP <sub>60</sub>	60.3 $\pm$ 6.1	98.6 $\pm$ 9.6*
DP <sub>120</sub>	70.3 $\pm$ 4.7	99.2 $\pm$ 6.1*
DP <sub>600</sub>	85.3 $\pm$ 2.1	99.7 $\pm$ 8.2*

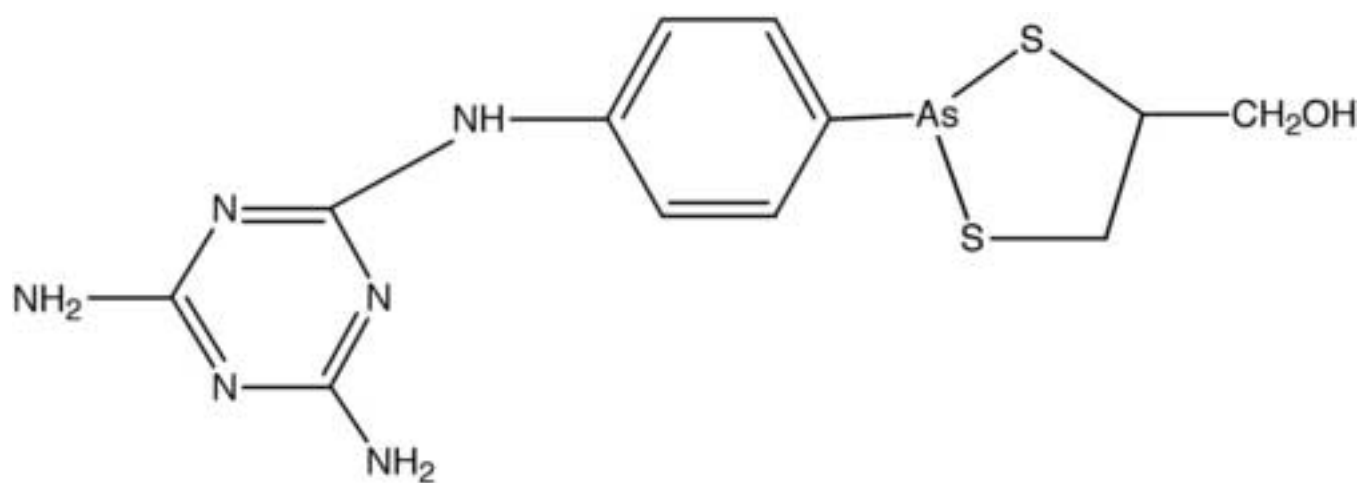
\* $P < 0.001$  versus free Mel ( $t$  test)

Table 5: Cytotoxicity parameters of free melarsoprol (Mel) and complexed with methyl  $\beta$ -cyclodextrin (Mel/RAME $\beta$ CD) on human cancer cell line U-937 and K562 (Trypan blue exclusion method; mean  $\pm$  S.D. n=3)

Cytotoxicity parameter	Mel		Mel/RAME $\beta$ CD	
	48 h	72 h	48 h	72 h
IC <sub>50</sub> ( $\mu$ M)	2.09 $\pm$ 0.08	2.40 $\pm$ 0.02	2.38 $\pm$ 0.44	3.16 $\pm$ 0.07 *
MC <sub>50</sub> ( $\mu$ M)	5.25 $\pm$ 0.38	4.25 $\pm$ 0.16	17.89 $\pm$ 4.84 *	4.45 $\pm$ 0.58

IC<sub>50</sub> : concentration inducing half-maximal inhibition; MC<sub>50</sub> : concentration inducing half-maximal mortality;  
 \*  $P < 0.01$  versus free melarsoprol (Mel)

Figure 1  
[Click here to download high resolution image](#)



$C_{12}H_{15}AsN_6OS_2$   
Mol. Wt.: 398,34

Figure 2  
[Click here to download high resolution image](#)

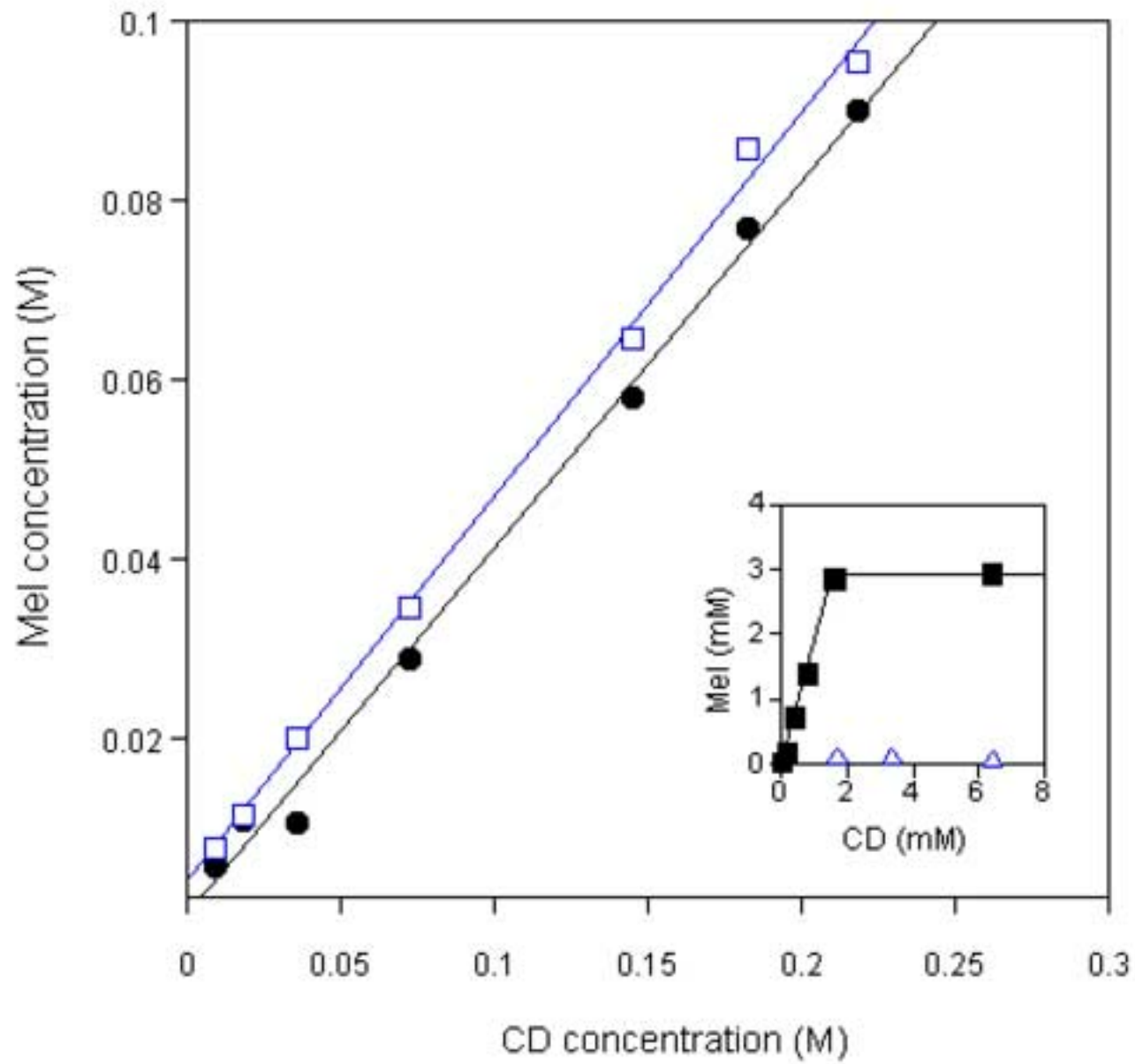




Figure 3  
[Click here to download high resolution image](#)

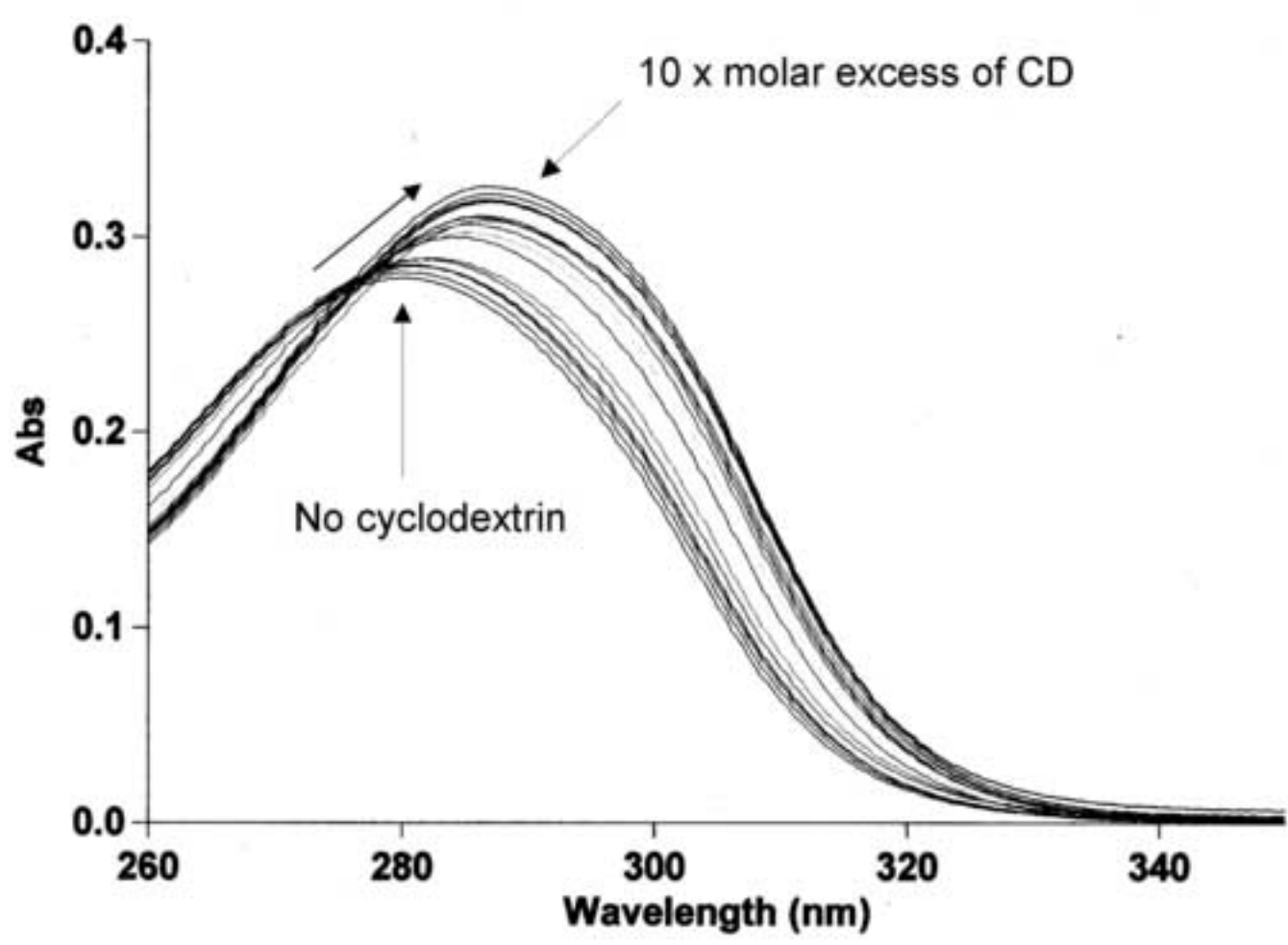


Figure 4  
[Click here to download high resolution image](#)

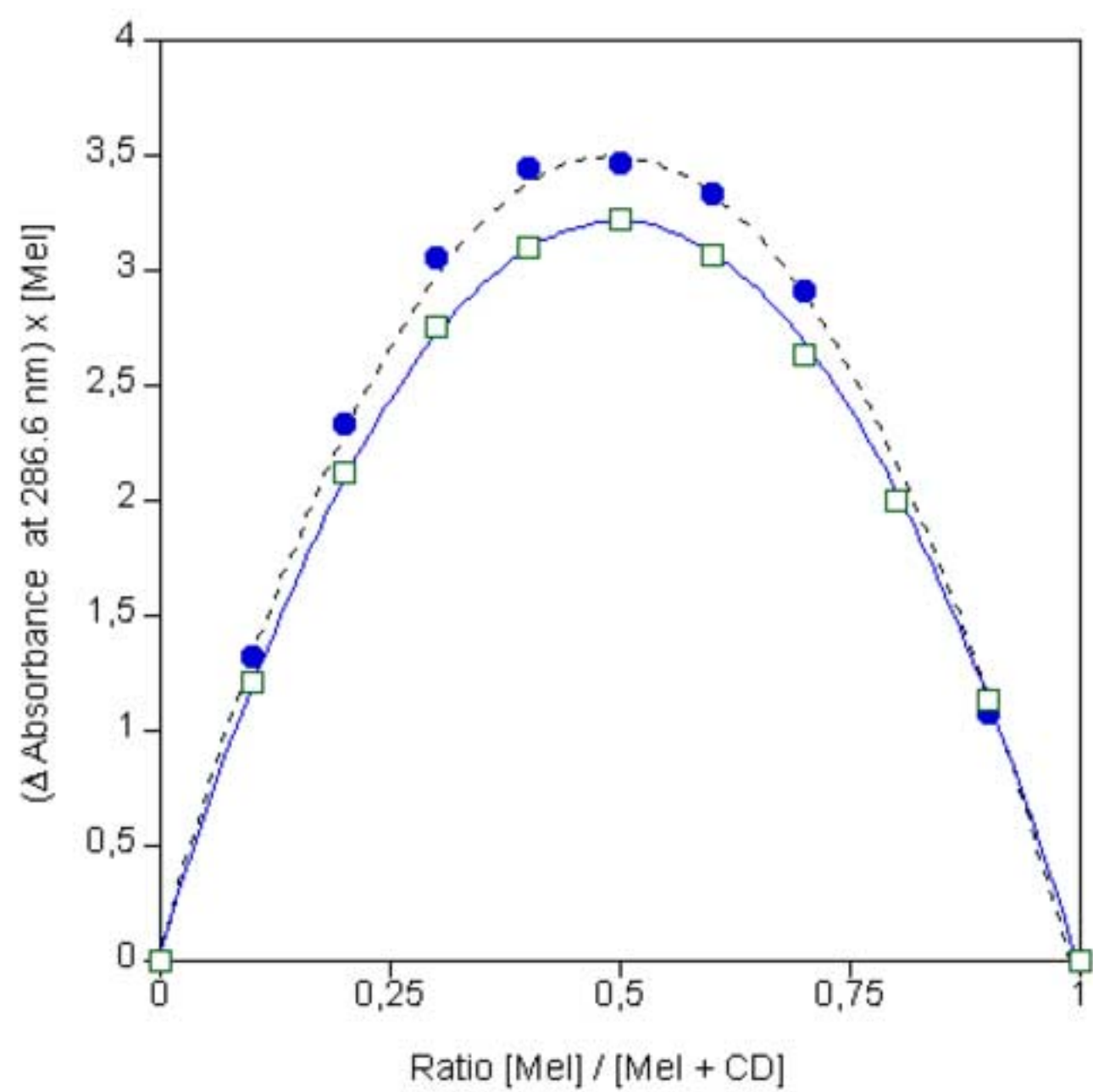


Figure 5  
[Click here to download high resolution image](#)

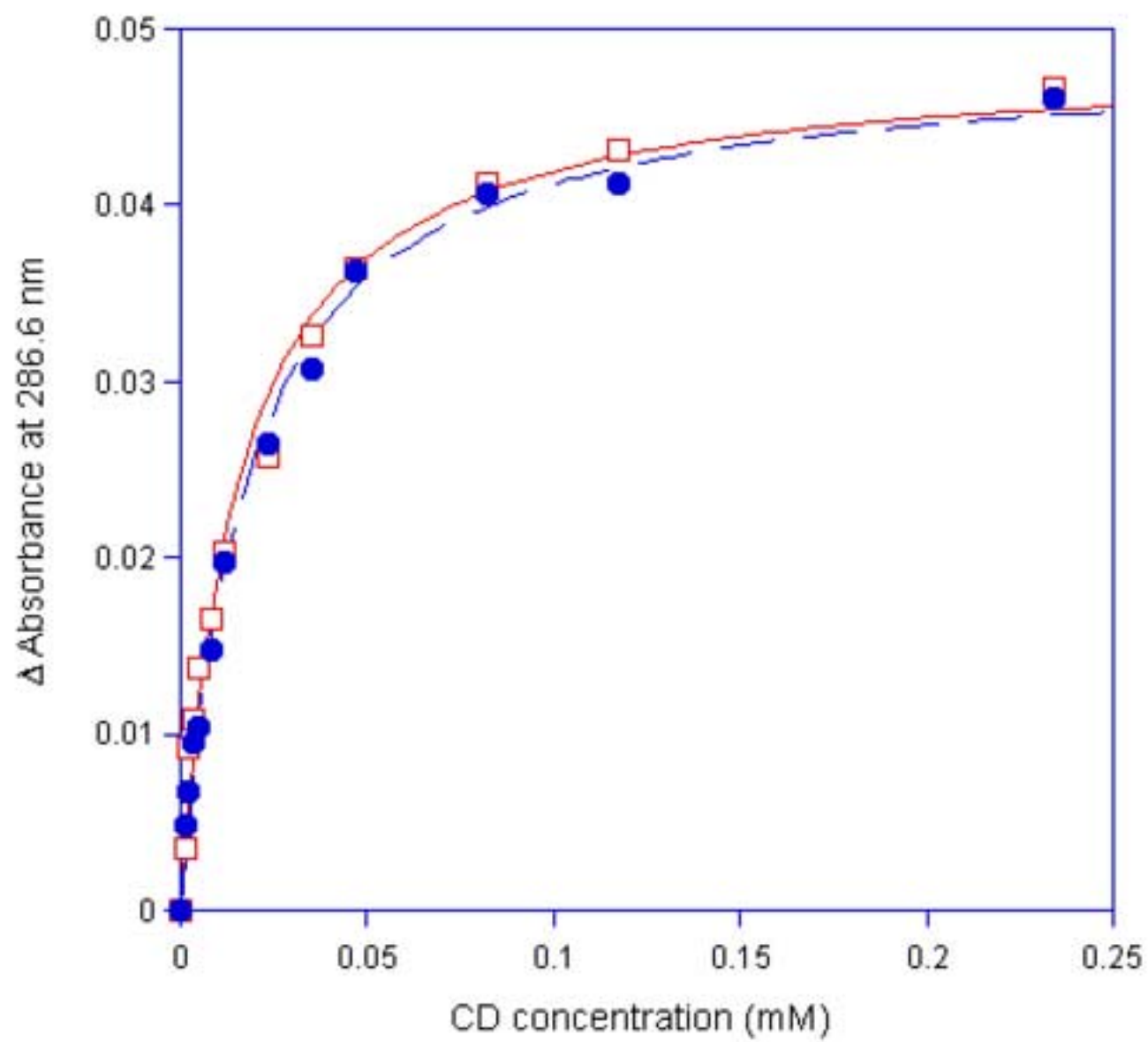
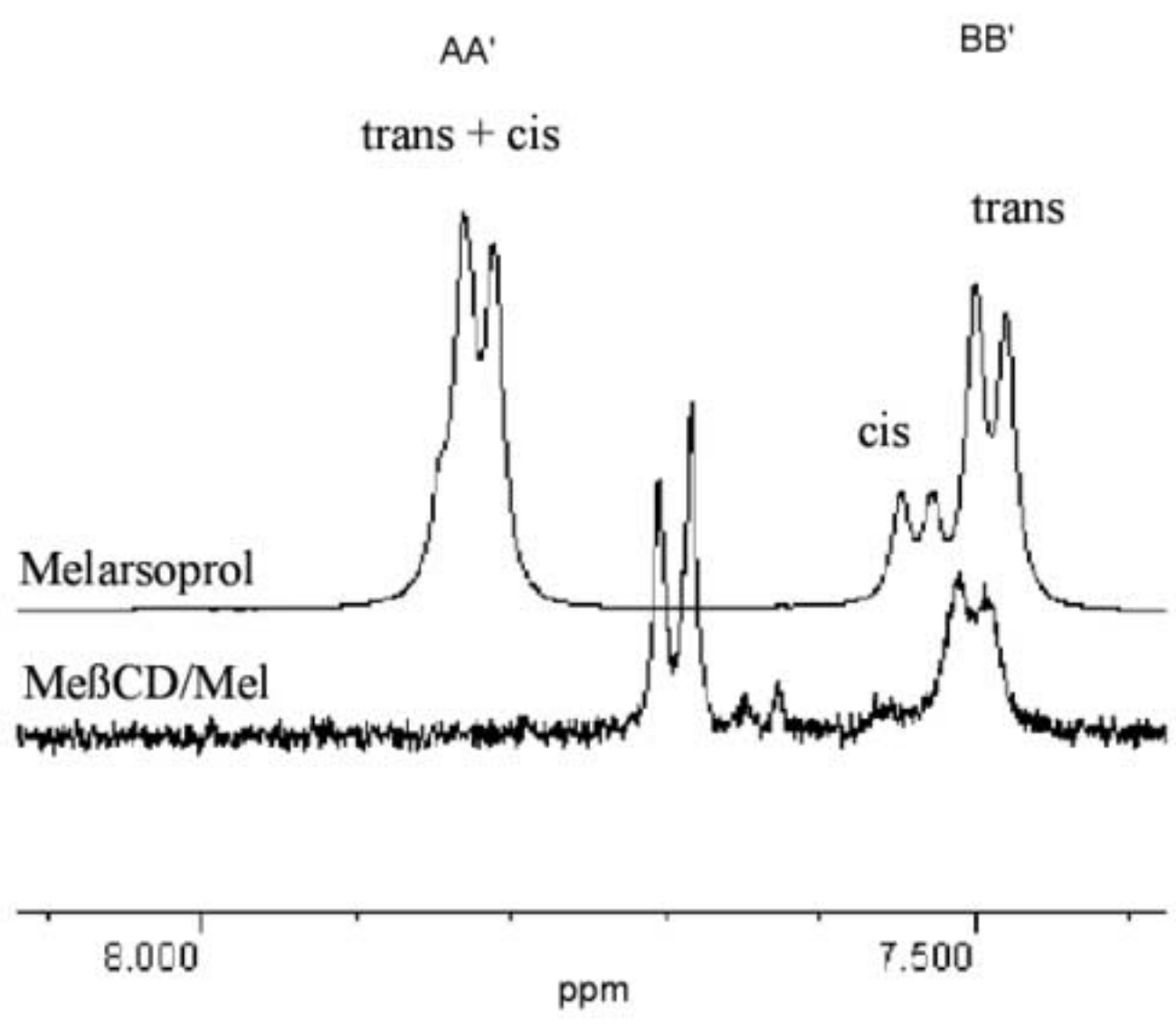
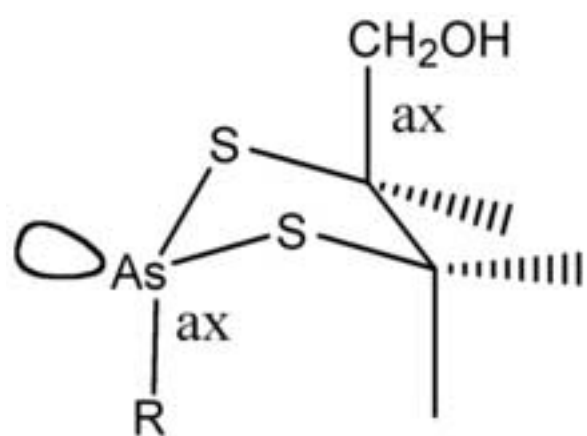
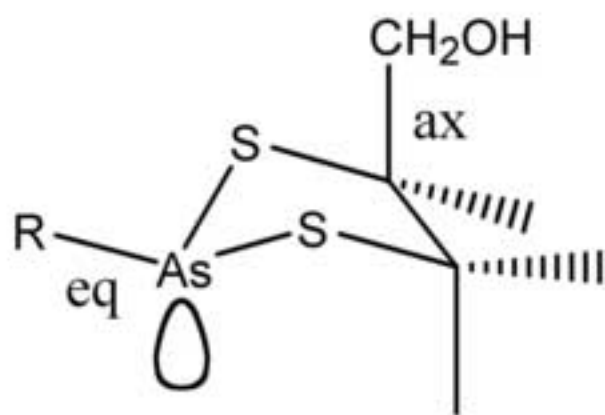


Figure 6  
[Click here to download high resolution image](#)





Major (75%)



Minor (25%)

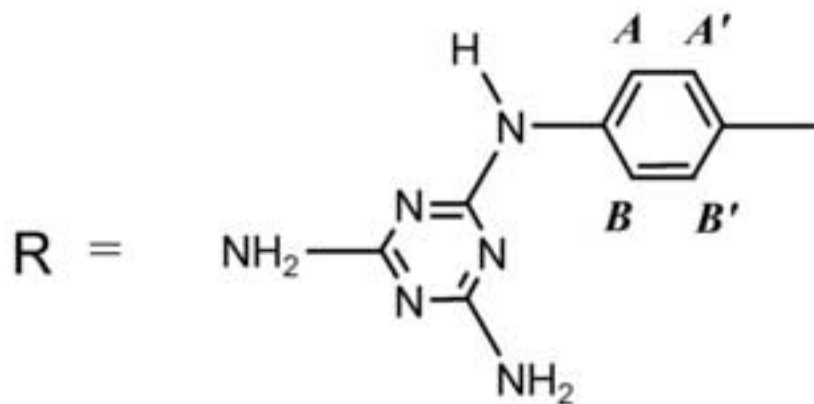


Figure 8

[Click here to download high resolution image](#)

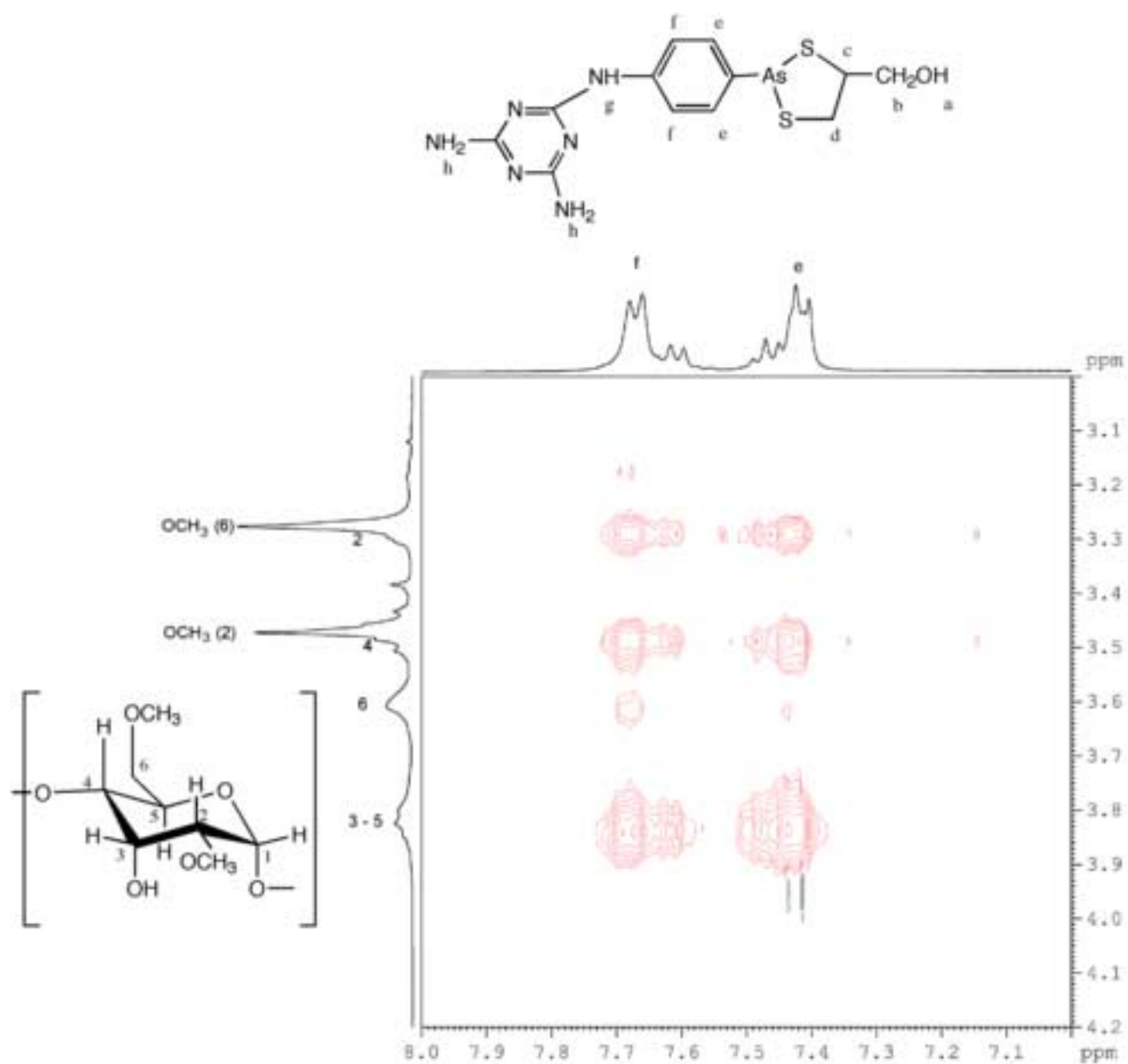


Figure 9  
[Click here to download high resolution image](#)

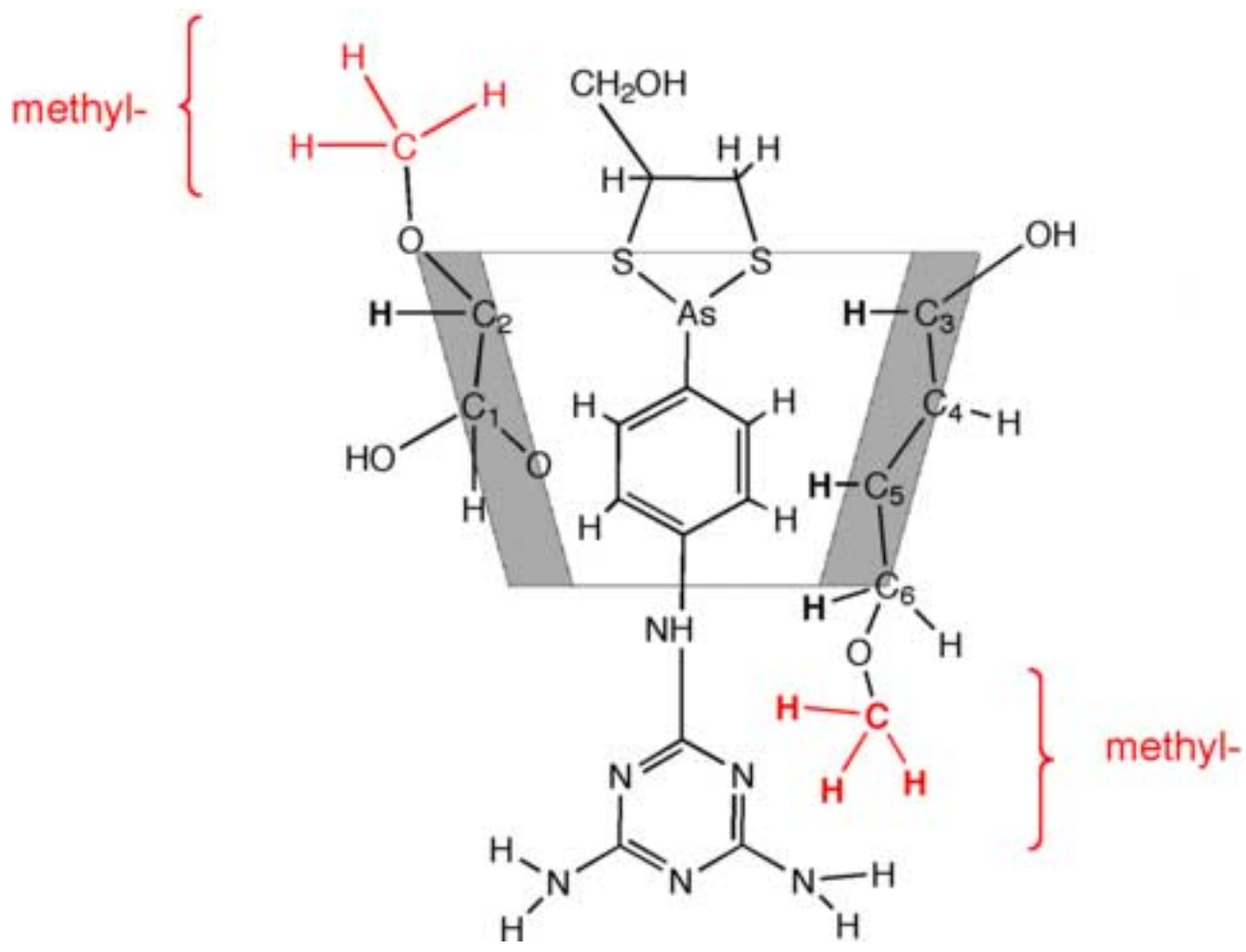


Figure 10  
[Click here to download high resolution image](#)

